

Experimental investigation of the temperature effect on the structural response of SG-laminated reinforced glass beams

Louter, Christian; Belis, J.; Bos, FP; Callewaert, D.; Veer, F.A.

DOI

[10.1016/j.engstruct.2010.02.007](https://doi.org/10.1016/j.engstruct.2010.02.007)

Publication date

2010

Document Version

Final published version

Published in

Engineering Structures

Citation (APA)

Louter, C., Belis, J., Bos, FP., Callewaert, D., & Veer, F. A. (2010). Experimental investigation of the temperature effect on the structural response of SG-laminated reinforced glass beams. *Engineering Structures*, 32(6), 1590-1599. <https://doi.org/10.1016/j.engstruct.2010.02.007>

Important note

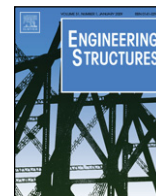
To cite this publication, please use the final published version (if applicable). Please check the document version above.

Copyright

Other than for strictly personal use, it is not permitted to download, forward or distribute the text or part of it, without the consent of the author(s) and/or copyright holder(s), unless the work is under an open content license such as Creative Commons.

Takedown policy

Please contact us and provide details if you believe this document breaches copyrights. We will remove access to the work immediately and investigate your claim.



Experimental investigation of the temperature effect on the structural response of SG-laminated reinforced glass beams

Christian Louter^{a,*}, Jan Belis^{b,2}, Freek Bos^{a,b,3}, Dieter Callewaert^{b,1}, Frederik Veer^{a,4}

^a Faculty of Architecture, Delft University of Technology, PO Box 5043, 2600 GA-Delft, The Netherlands⁵

^b Department of Structural Engineering – LMO, Ghent University, Technologiepark-Zwijnaarde 904, B-9052 Ghent, Belgium⁶

ARTICLE INFO

Article history:

Received 18 September 2009

Received in revised form

25 January 2010

Accepted 1 February 2010

Available online 5 March 2010

Keywords:

Structural glass

Reinforced glass

SentryGlas interlayer

Laminate

Temperature effect

Experiment

Failure analysis

ABSTRACT

To generate high-level redundancy for structural glass beams, a novel concept of laminating a metal reinforcement to a structural glass beam has been developed at Delft University of Technology (TU Delft). This concept makes use of the relatively stiff polymer interlayer material SentryGlas (SG) to bond the metal to the glass. However, due to the visco-elastic properties of the SG, its stiffness varies at different temperature levels. To what extent this temperature dependency has an effect on the structural response of the beam composite has been experimentally investigated in cooperation with Ghent University (UGent) and is the subject of current publication. Two separate series of pull-out tests, to investigate the bond strength, and beam tests, to investigate the post-breakage response, have been conducted at -20 , 23 and 60 °C. The pull-out tests revealed a high temperature dependency of the bond strength of SG. This temperature dependency also had an effect on the structural response of the beams. However, regardless of temperature level all beams showed high-level plastic response and high redundancy. It is therefore concluded that temperature levels of -20 to 60 °C do not endanger the structural safety of SG-laminated reinforced glass beams.

© 2010 Elsevier Ltd. All rights reserved.

1. Introduction

Applications of load-bearing glass beams and fins are frequently present and rapidly developing in contemporary architecture. In spite of this evolution, the safety concepts which are generally used for such load-bearing components are based on basic concepts adopted from conventional window glazing, such as laminating glass to glass by means of a polymer interlayer. However, whereas these laminating concepts provide sufficient safety for conventional window glazing, they do not always provide an acceptable safety level for structural glass beams. Even when a relatively stiff interlayer polymer is used, such as the ionomer interlayer SentryGlas (SG), the safety level and residual load-bearing capacity of laminated structural glass beams remain limited as has been shown by Belis et al. [1], Delincé et al. [2] and Bos [3].

* Corresponding author. Tel.: +31 15 2781115.

E-mail addresses: p.c.louter@tudelft.nl, paper@pclouter.nl (C. Louter).

¹ Research Engineer and Doctoral Candidate.

² Lecturer.

³ Postdoctoral researcher.

⁴ Senior Lecturer.

⁵ www.glass.bk.tudelft.nl.

⁶ www.LMO.UGent.be.

In search for a better safety concept, several authors have reported on an advanced approach, based on a composite action between glass and an incorporated metal reinforcement. Feirabend [4] investigated the post-failure behaviour of glass laminates with a metal wire-mesh or perforated sheet embedded in the interlayer. Belis et al. [5] reported on a hybrid beam system combining a glass web with a small, adhesively bonded steel frame. Finally, Louter, Veer et al. and Bos developed a glass beam concept with incorporated metal reinforcements [6–8]. Similar to reinforced concrete, the latter concept makes use of the elasto-plastic properties of the metal reinforcement to generate safe and ductile failure with a significant residual load-bearing capacity. Up to a significant extent, tensile stresses are supposed to be taken directly by the glass; the reinforcement is only fully developing its potential after one or more glass plates are broken.

Originally developed with acrylic adhesives, the reinforced glass beam concept is recently evolving more towards polymer-film based technology [9]. More specifically, recent studies [10] pointed out the promising metal-to-glass bonding properties of SG polymer interlayers, used for example in some of the well-known all-glass staircases of Apple stores all over the world [11].

However, due to the visco-elastic properties of most polymer interlayers, their shear stiffness varies at different temperature levels. Up until now, it is unknown to what extent this temperature dependency effects the structural response of the overall beam

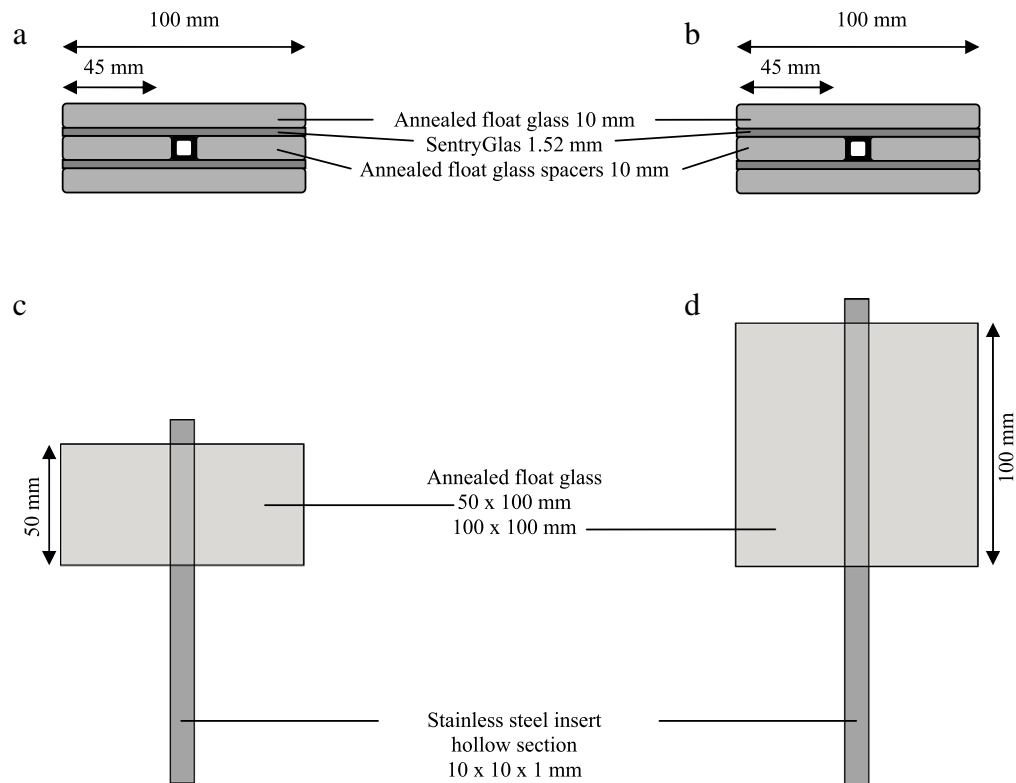


Fig. 1. Geometry of tests specimens for pull-out tests: (a, b) top view series 50 and 100 mm respectively, (c, d) side view series 50 and 100 mm respectively.

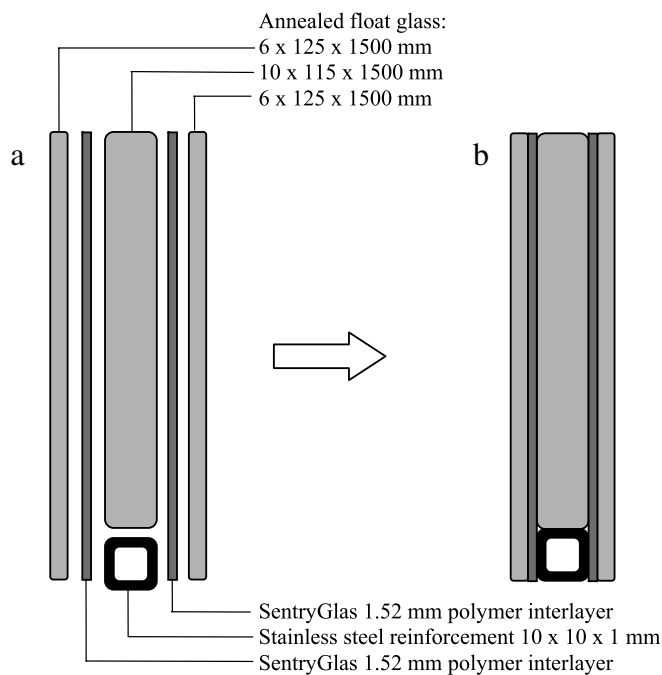


Fig. 2. Cross-section of reinforced laminated glass/SG beam specimens: (a) exploded view, (b) assembled view.

composite. Consequently, the current study investigates the temperature effect on the structural response. To do so, an experimental approach is used, enabling the comparison and integration of small-scale pull-out test results and medium-scale four-point bending test results at -20 , 23 and 60 °C. This study forms an extension to the results published by Louter et al. in [12,13].

2. Test specimens

The following sections will describe the applied materials and the geometry of both the pull-out and beam specimens. For the pull-out specimens, which consist of a small glass laminate with a metal insert, two series of nine specimens with a varying bond length of 50 or 100 mm have been made, see Table 1. For the beams, which consist of a glass laminate with a metal reinforcement laminated at the edge subjected to tensile stresses, a total of 15 equal specimens have been made, see Table 1.

2.1. Materials

The main properties of all used materials are listed in Table 2.

For the glass an ordinary annealed float glass has been used, which has been cut and ground by a commercial supplier. The glass has not been tempered since this would result in a more extensive fracture pattern which might possibly limit the post-breakage strength of the reinforced glass beams [18].

For all metal inserts standard and commercially available stainless steel type 304L has been applied. It has been applied as a hollow section with section dimensions $10 \times 10 \times 1$ mm. No special surface treatment has been applied to the stainless steel.

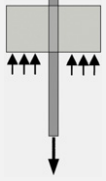
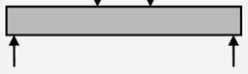
The polymer interlayer used to adhesively bond glass to glass and glass to metal was SentryGlas (SG), also referred to in literature as ionomer or “ionoplast” interlayer [16]. In this study, 1.52 mm thick SG sheets have been used in a conventional laminating cycle to produce the test samples.

Prior to assembly the glass and stainless steel have been cleaned with 2-propanol. All specimens have been made with the tin side of the outer glass sheets facing the metal inserts.

2.2. Pull-out test specimens

The geometry of the pull-out specimens is illustrated in Fig. 1. Both the 50 mm and 100 mm specimens have been composed of

Table 1
Overview of the amount of specimens per test type and per test temperature.

	Stainless steel insert	Pull-out specimens		Beam specimens
		50 mm	100 mm	
				
–20 °C	–	3	3	5
23 °C	3	3	3	5
60 °C	–	3	3	5
Total	3	9	9	15

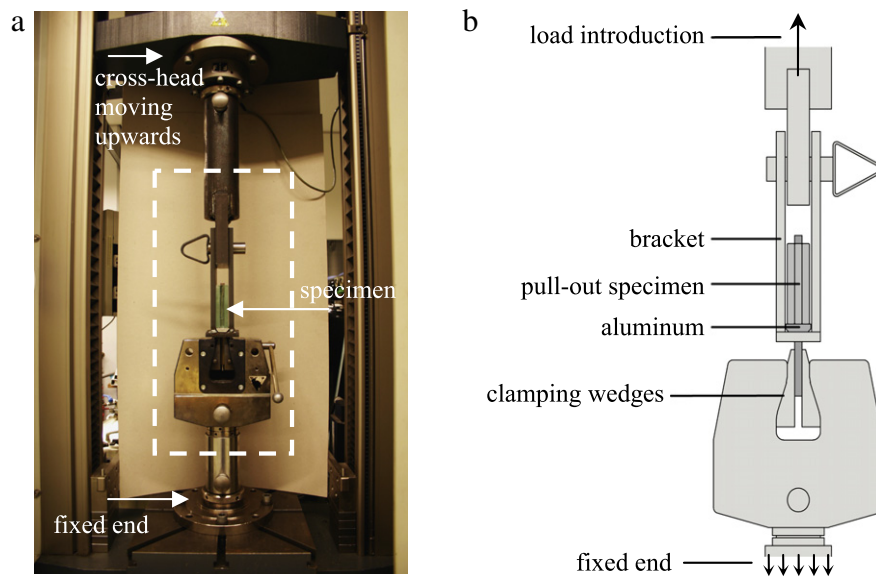


Fig. 3. (a) Photograph of the pull-out test setup. (b) Schematic representation of the pull-out test setup.

Table 2
Indicative mechanical properties of annealed glass [14], stainless steel [15] and SentryGlas [16,17].

Property	Unit	Glass annealed	Interlayer sentryGlas	Stainless steel 304L
Tensile strength	N/mm ²	45	34.5	500–720 (at 20 °C)
Elastic modulus	N/mm ²	70×10^3	493 (at 20 °C) ^a	200×10^3 (at 20 °C)
Glass transition temperature	°C	N/A	~55–60	N/A
Elongation at tear	%	–	400	45
Density	kg/m ³	2500	950	7900 (at 20 °C)
Coefficient of thermal expansion	K ⁻¹	9×10^{-6} (20–300 °C)	$10\text{--}15 \times 10^{-3}$	16.5×10^{-6} (20–200 °C)

^a Value for a load duration of one hour according to Stelzer and Bennisson [16].

three 10 mm thick annealed glass layers, two 1.52 mm thick SG interlayers and a metal insert. The middle glass layer has been split in two parts, called the spacers, to host the $10 \times 10 \times 1$ mm stainless steel hollow section insert. The assembled sandwich elements of glass, SG and stainless steel have been laminated by commercial suppliers in a standard laminating cycle.

Prior to the pull-out tests the specimens have been conditioned for several days. The specimens tested at room temperature had been conditioned for 1 week at 23 °C (± 1 °C) in the same room as the test setup. The specimens tested at –20 °C had been conditioned for 1 week at –23 °C (± 1 °C) in an ordinary refrigerator. The specimens tested at 60 °C have been conditioned for 5 days in an oven at 63 °C (± 1 °C).

2.3. Beam test specimens

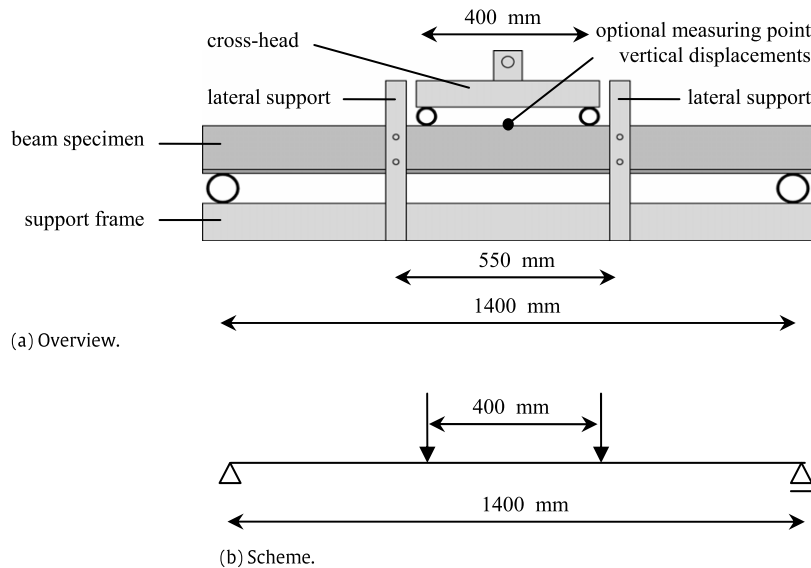
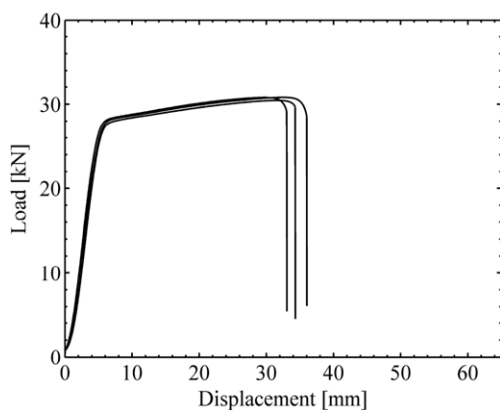
The geometry of the beam specimens is illustrated in Fig. 2. The beam specimens consisted of two outer glass layers and one inner glass layer with a cross-section of 6×125 mm and 10×115 mm respectively, a $10 \times 10 \times 1$ mm stainless steel hollow section positioned at the edge of the inner glass layer and two 1.52 mm thick SG sheets acting as adhesive interlayers. The assembled beam composites have been laminated by a commercial supplier in a conventional vacuum bag process.

Prior to the bending tests the beam specimens had been conditioned for several days. The beams tested at room temperature had been conditioned for 1 week at 23 °C (± 1 °C) in the same room as

Table 3

Mean values and standard deviations of pull-out and uniaxial tensile test results.

	Units	50 mm pull-out specimens			100 mm pull-out specimens		
		23 °C	−20 °C	60 °C	−20 °C	23 °C	60 °C
Maximum load							
Mean	kN	30.7	24.2	21.8	10.5	30.1	12.4
St.dev.	kN	0.2	4.3	1.2	12.2	1.4	0.5
Rel.st.dev.	%	0.7	17.8	5.3	10.7	4.6	3.8
Residual resistance							
Mean	kN	–	0.6	0.8	1.8	3.0	5 ^a
St.dev.	kN	–	0.4	0.9	1.1	3.8	–
Rel.st.dev.	%	–	67.8	115.4	62.7	3.1	–

^a Based on one test. The other tests had been stopped prematurely.**Fig. 4.** (a) Overview and (b) schematic representation of the four-point bending test setup.**Fig. 5.** Load–displacement diagrams of uniaxial tensile tests on the metal inserts.

the test setup. The beams tested at $-20\text{ }^{\circ}\text{C}$ had been conditioned for one week in a refrigerator at $-30\text{ }^{\circ}\text{C}$ ($\pm 3\text{ }^{\circ}\text{C}$). The conditioning temperature was chosen $10\text{ }^{\circ}\text{C}$ lower than the testing temperature to compensate for any heat gain during transportation and mounting of the beam specimens, which took about five minutes per specimen.

The beam specimens selected for testing at $60\text{ }^{\circ}\text{C}$ were stored for at least 36 h at $60\text{ }^{\circ}\text{C}$. Since both conditioning and testing took place in the same climatic chamber, no temperature difference occurred due to transportation and mounting of these specimens.

3. Test methods

The following sections will describe the test procedures followed for both the pull-out and beam tests. The high temperature beam tests have been conducted at Ghent University. The remaining tests have been conducted at Delft University of Technology.

3.1. Pull-out tests

The pull-out tests have been performed at -20 , 23 and $60\text{ }^{\circ}\text{C}$ on a Zwick Universal 100 kN testing machine. The stainless steel insert of the specimens was clamped in the lower clamping wedges of the testing machine, as illustrated in Fig. 3, upon which the upper steel bracket containing the glass laminate was moved upwards at a fixed displacement rate of 2 mm/min . Consequently, the metal insert was pulled out of the glass laminate. During the tests the load

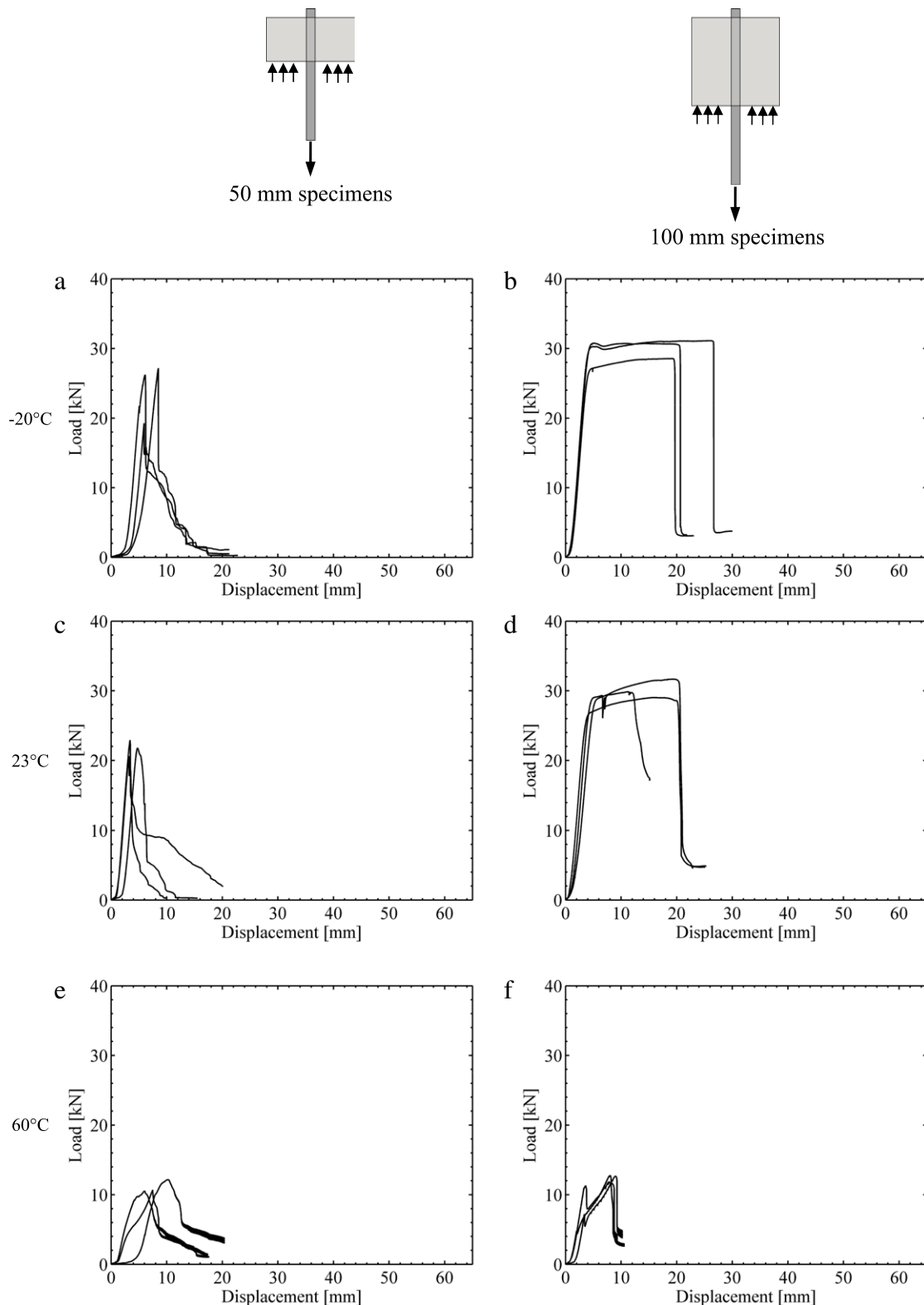


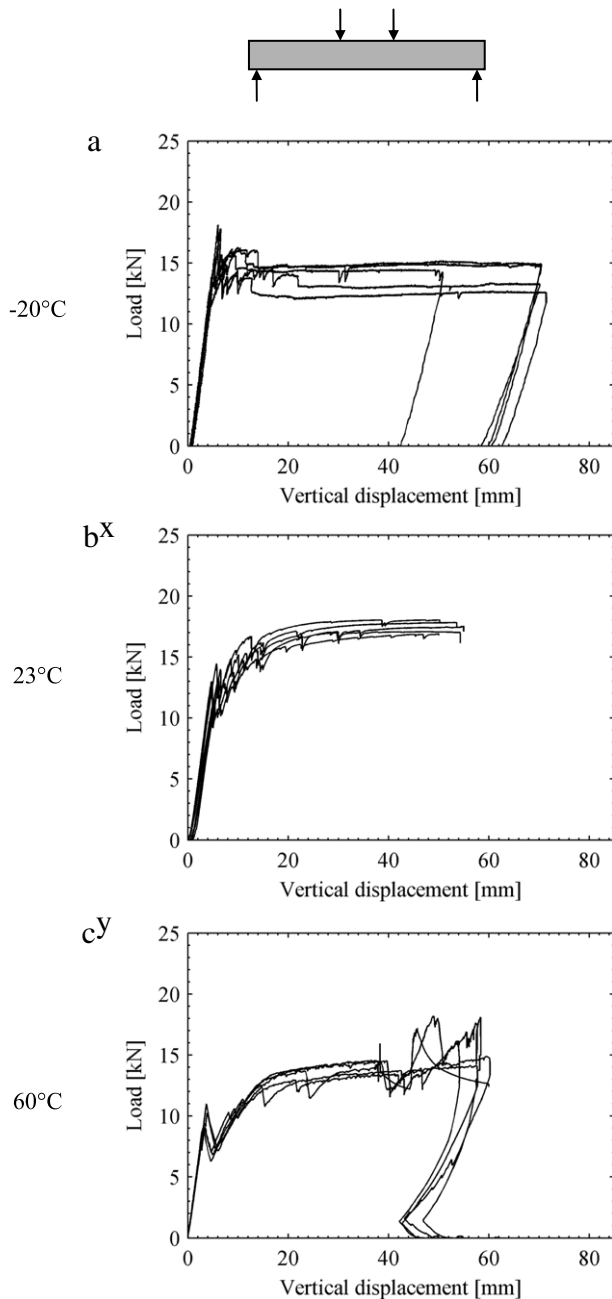
Fig. 6. Load–displacement diagrams of pull-out tests: (a, b) at -20 , (c, d) at 23 and (e, f) at 60 °C.

and the displacement of the cross-head, see Fig. 3(a), have been measured.

For the pull-out tests at lower and higher temperatures (-20 and 60 °C respectively) an insulated climatic box has been positioned around the test setup. This climatic box has been either cooled with vaporized liquid nitrogen or heated with an electric heating element. A fan at the back side of the climatic box

generated an air flow throughout the climatic box which ensured an even temperature level throughout the climatic box.

As a reference, additional uniaxial tensile tests have been performed at room temperature on the stainless steel inserts only. The same testing conditions have been applied as in the pull-out tests.



^x The tests at 23 °C had been stopped at about 55 mm displacement.

^y At the end of the loading procedure the load-displacement diagram shows some sudden increases in load, caused by a rapid increase of the applied displacement rate. These load peaks, however, should be disregarded in the further analysis of the test results.

Fig. 7. Load–displacement diagrams of four-point bending tests at –20, 23 and 60 °C.

3.2. Beam tests

Three series of five beam specimens each have been destructively investigated in four-point bending tests at either –20, 23 or 60 °C. Regardless of the testing temperature, the span was the same for all four-point bending tests, according to the values shown in Fig. 4. During all bending tests the applied load and the vertical displacement of either the cross-head or the vertical displacement at mid-span of the beam, see Fig. 4(a), have been measured.

Table 4

Mean values and standard deviations of four-point bending test results at –20, 23 and 60 °C.

		–20 °C	23 °C	60 °C
	Units			
Initial failure load				
Mean	kN	16.1	11.7	9.1
St. dev.	kN	1.8	1.1	1.3
Rel. st. dev.	%	11.2	9.5	14.4
Residual load				
Mean	kN	15.4	17.5	14.3
St. dev.	kN	0.9	0.5	0.5
Rel. st. dev.	%	5.6	2.8	3.7
$\frac{\text{Residual load}}{\text{Initial load}} \times 100\%$				
Mean	%	96.4	150	159.1
St. dev.	%	7.7	12.0	22.7
Rel. st. dev.	%	7.9	7.7	14.2

During the bending tests at room temperature (23 °C), a vertical displacement rate of 2 mm/min was used until initial glass breakage occurred. Subsequently, the load was removed in order to investigate the fracture pattern. Finally, the specimens were loaded in a second test run at a rate of 5 mm/min.

The lower testing temperature, realised in a small-scale climatic box mounted on the testing machine and cooled with vaporized liquid nitrogen, was manually targeted at –20 °C (± 5 °C). At this temperature, a single vertical displacement rate of 2 mm/min was used.

Finally, the bending tests at 60 °C were performed in a large-scale climatic chamber. In the test setup the load was applied using a hydraulic jack. The vertical displacement rate was manually controlled by increasing the oil pressure using a hydraulic vessel.

4. Results

4.1. Pull-out test results

As a reference for the pull-out tests discussed below, load–displacement diagrams of the uniaxial tensile tests on the stainless steel inserts are presented in Fig. 5. Subsequently, mean values and standard deviations of pull-out and uniaxial tensile test results are presented in Table 3. Finally, Fig. 6 shows the corresponding load–displacement diagrams of the pull-out tests at all tested temperatures. The results will be discussed in Section 5.1.

4.2. Bending test results

The results of the bending tests are presented in Fig. 7, which provides the load–displacement diagrams, and Table 4, which provides the most important values. The results will be discussed in Section 5.2.

5. Discussion

5.1. Pull-out tests

The results of the pull-out tests showed differences in bond strength at the different test temperatures, differences in failure mode and differences between the 50 and 100 mm specimens. These aspects are discussed in the following subsections.

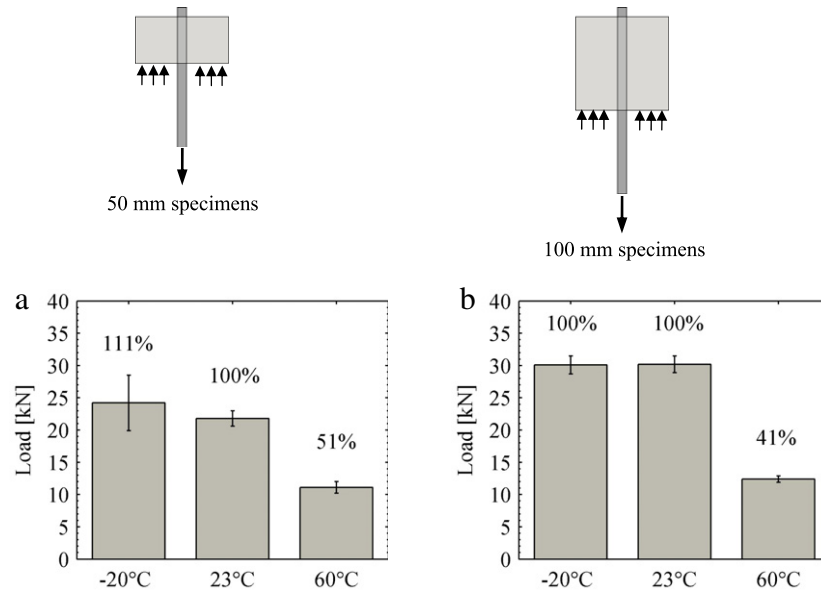


Fig. 8. Bar graph of the mean pull-out loads per specimen type at -20 , 23 and 60 °C. The mean load value at 23 °C has been set as a reference of 100% for each series.

5.1.1. Influence of testing temperature

The results of the pull-out tests clearly show a temperature dependency of the bond strength of the SG interlayer. Compared to room temperature (23 °C) the bond strength drastically drops at 60 °C, as can be seen in Fig. 8. At -20 °C a slight increase in bond strength of the SG compared to room temperature was observed for the 50 mm pull-out specimens, see Fig. 8(a). The fact that this increase in maximum pull-out strength is absent for the 100 mm specimens, see Fig. 8(b), originates from the limited tensile capacity of the metal insert as will be further explained in Section 5.1.3.

The observed negative influence of higher testing temperatures on the metal-to-glass bond strength of the SentryGlas (SG) interlayer can be explained by the SG glass transition temperature of ~ 55 – 60 °C, see Table 2, which corresponds approximately to 60 °C applied during the tests. At this temperature level the polymer stiffness and shear modulus of the SG interlayer is drastically reduced, which will limit the shear transfer capacity of the SG interlayer.

Reversibly, the observed increase in bond strength at -20 °C can be explained by an increase in polymer stiffness and shear modulus of the SG interlayer at lower temperature levels. However, it should be noted that the scatter in the result of the 50 mm specimens tested at -20 °C is relatively large, which urges for caution in interpreting these results. Further study will therefore be necessary to confirm the tendency of increasing bond strength of the SG at lower temperature levels.

5.1.2. Failure modes

As a consequence of the temperature-dependency discussed above, the failure mode of the pull-out test specimens depended on the testing temperature as well.

More specifically, glass fracture was observed during all tests at -20 and 23 °C, as illustrated by the failed specimens in Fig. 9(a), (b), (c) and (d). This glass breakage was most probably caused by the relatively high shear stiffness of the SG, see Table 2, and the consequent very good load transfer to the glass at these temperatures.

However, no glass fracture occurred during the tests at 60 °C, as illustrated in Fig. 9(e) and (f). Apparently, the shear stiffness of the SG was reduced sufficiently to allow a friction-slip displacement

of the stainless steel insert. The authors assume that this friction is generated by an interlocking effect of the failed interlayer remainders.

5.1.3. Influence of test specimen geometry

The test results of the pull-out tests also revealed some differences between the 50 and 100 mm specimens.

The first difference between the 50 and 100 mm specimens regards their maximum pull-out capacity. At all temperature levels the 100 mm specimens show higher pull-out strength values than the 50 mm specimens, see Table 3 or Fig. 8. This difference originates from the increased bond length of the 100 mm specimens, which effectively increases the load transfer capacity between the metal insert and the glass through shear in the SG interlayer. For the 100 mm pull-out specimens tested at -20 and 23 °C the increased load transfer capacity was even sufficient to cause yielding of the metal insert. This explains the horizontal yielding trajectory in the load–displacement diagrams of the 100 mm pull-out specimens tested at -20 and 23 °C which are absent for the 50 mm pull-out specimens, see Fig. 6. When the load–displacement diagrams of the 100 mm -20 and 23 °C pull-out tests, see Fig. 6(b) and (d), are compared with the load–displacement diagrams of the uniaxial tensile reference tests on the stainless steel inserts, see Fig. 5, the resemblance is striking. Consequently, it is concluded that the maximum pull-out strength of the 100 mm specimens at -20 and 23 °C was governed by yielding of the metal insert. This also explains that for the 100 mm specimens there is no difference in maximum pull-out strength between the -20 and 23 °C test, whereas this difference indeed has been observed for the 50 mm specimens, see Section 5.1.1 and Fig. 8.

The second difference between the 50 and 100 mm specimens regards their residual pull-out resistance. This difference can be derived from the load–displacement diagrams of the 50 and 100 mm at -20 and 23 °C, see Fig. 6(a) and (b) or (c) and (d). Whereas the 100 mm specimens demonstrate at the end of the loading procedure a residual pull-out resistance up to 5 kN, see Table 3, the 50 mm specimen show a gradual drop in pull-out resistance towards 0 kN without a significant residual pull-out capacity. This difference was probably caused by two aspects. Firstly, the residual bonding surface for the 50 mm was limited compared to the 100 mm specimens, which limited their residual

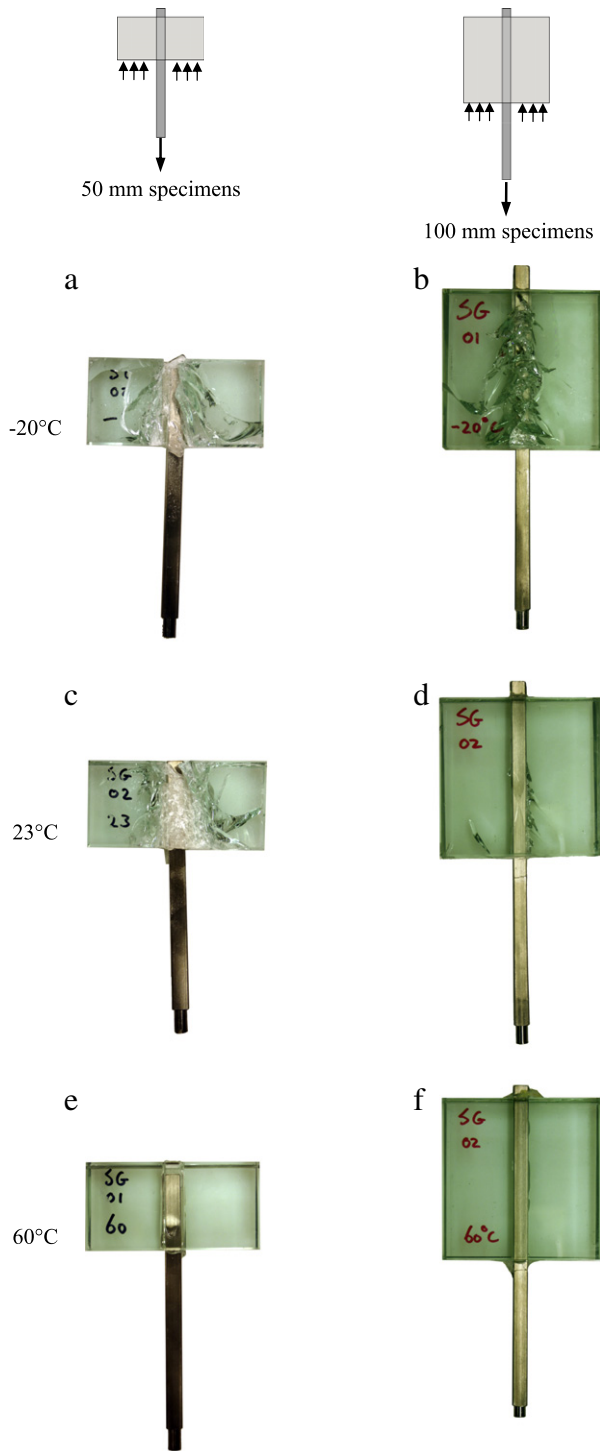


Fig. 9. Examples of failed pull-out test specimens of 50 and 100 mm at -20 , 23 and 60 °C.

friction capacity. Secondly, the 50 mm specimens showed more extensive cracking upon glass failure than the 100 mm specimens, see Fig. 9(a) and (b) or (c) and (d), which also limited their residual friction capacity.

At 60 °C the differences in residual pull-out capacity and maximum pull-out capacity between the 50 and 100 mm is smaller than at -20 and 23 °C. Due to a decreased shear modulus of the SG interlayer at 60 °C the load transfer capacity of both the 50 and 100 mm specimens has drastically reduced. This reduced shear modulus has evened out any differences between the 50 and 100 mm specimens.

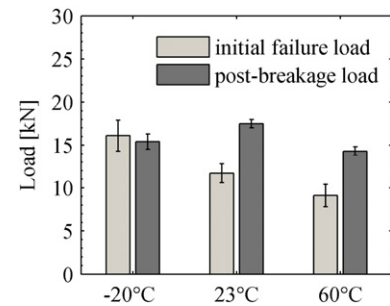


Fig. 10. Bar graph of the mean initial and post-breakage load of the beam specimens tested at -20 , 23 and 60 °C.

5.2. Bending tests

As can be seen in Fig. 7, all tested beams revealed an initial linear response until the first glass breakage, followed by a relatively high-level plastic behaviour which is frequently disrupted by temporary local drops in load caused by additional cracks in the glass.

In general the results of the bending tests performed at -20 , 23 and 60 °C on SG-laminated metal-reinforced glass beams showed that laminating a metal reinforcement to a structural glass beam using SG is a feasible and promising concept, which generates a high level of redundancy even at extreme temperature conditions. The metal-to-glass bond, generated by the SG interlayer, is strong enough to transfer the forces between glass and reinforcement once the glass has cracked and the reinforcement is activated. However, significant differences in the structural response at -20 , 23 and 60 °C have been observed with respect to the initial glass breakage loads and the post-breakage behaviour.

5.2.1. Initial glass breakage loads

The initial glass breakage loads differed significantly for the different testing temperatures, see Fig. 10. The beams tested at room temperature had a mean initial failure load of 11.7 kN, whereas the specimens tested at -20 and 60 °C had a mean initial failure load of 16.1 kN and 9.1 kN respectively. Although this difference is theoretically in line with an increased stiffness of the SG at low temperature levels and a decreased stiffness at increased temperature levels, it seems unlikely that the SG has contributed this significantly to the difference in initial load carrying capacity. Since the elastic modulus of SG, which is 493 N/mm² for a load duration of one hour at 20 °C according to Table 2, is relatively low compared to the Young's modulus of glass, which is $70\,000$ N/mm², it is assumed that the bending stiffness of the SG contributed only to a negligible extent to the initial load carrying capacity. It seems more likely that the differences in initial strength originate from the level of activation of the stainless steel reinforcement. More specifically, the results of the pull-out tests discussed above clearly demonstrated the very good shear load transfer between glass and stainless steel at -20 and 23 °C. In addition and in perfect accordance with the findings of the pull-out tests, the contact area between reinforcement, SG and glass was relatively large in the beam bending tests, which is very favourable for load transfer as well. Summarizing, the authors suggest that the relatively high load values obtained at -20 and 23 °C are at least partially due to the stainless steel reinforcement, which was originally meant for post-failure safety but which is activated before failure as well by high shear load transfer capabilities of the SG interlayer, partially taking over tensile bending stresses acting on the glass.

To some extent, other effects might have played a minor role, such as a difference in sub-critical crack growth in the glass, which is dependent on the temperature [19], differences in relative humidity during storage and testing, or additional surface flaws due to extra transportation and manipulation for the tests at 60 °C.

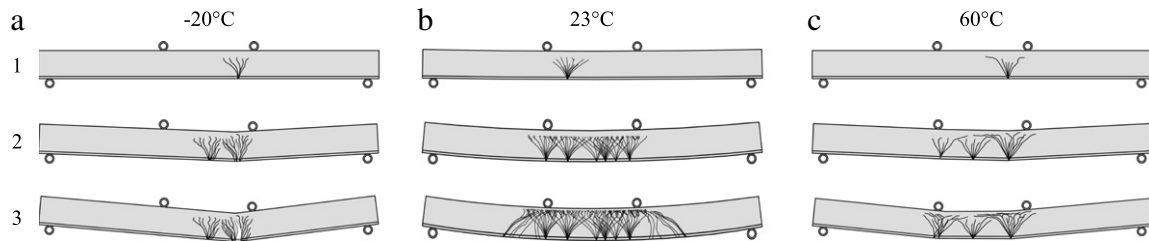


Fig. 11. Crack development in the beam specimens tested at -20 , 23 and 60 °C. (1) primary cracking (at high speed) of one of the outer sheets; (2) secondary cracking (at high speed) and crack propagation (slow propagation) at multiple sheets; (3) final stage.

5.2.2. Post-breakage performance and failure modes

The beams showed their best post-breakage performance at 23 °C, see Fig. 10. At this temperature the bond strength between reinforcement and glass was sufficient to effectively activate the reinforcement. Although some minor and local delamination and consequent debonding of reinforcement occurred upon initial glass failure, the cracks in the glass were most effectively arrested by the reinforcement. Subsequent yielding of reinforcement provided a highly plastic post-breakage beam response, see Fig. 7(b). Furthermore, the beams tested at room temperature profited from an additional load carrying mechanism, which was absent for the beams tested at -20 and 60 °C. As suggested by Bos in [3], an additional load carrying mechanism in SG-laminated beams is generated by glass fragments of one pane overlapping local cracks in the other. Since the SG interlayer acts as a crack barrier, a crack will only affect one glass layer of the beam laminate. The other layers will remain locally unaffected and will bridge the crack, thereby transferring bending induced forces through shear in the SG interlayer. As long as cracks do not coincide, which is initially prevented by the crack stopping properties of the SG interlayer, the overlapping glass segments provide a significant additional load carrying capacity. As will be discussed below this additional load-carrying mechanism is absent for the beams tested at -20 and 60 °C due to the occurrence of plastic hinges in the beams as a result of decreased fracture toughness and decreased bond strength of the SG at -20 and 60 °C respectively.

At -20 °C the beams showed reduced post-breakage performance compared to 23 °C. At -20 °C more excessive delamination and debonding of reinforcement occurred upon initial glass failure than at 23 °C. Since the bond strength of the SG had not decreased at -20 °C, as has been observed in the pull-out tests, the increased delamination probably originates from decreased fracture toughness of the SG interlayer at -20 °C. A similar effect of delamination between glass and polymer at low temperature has also been observed by Meissner and Bucak [20] on a prior generation of SG. Due to this local debonding in the SG beams the reinforcement could less effectively arrest the cracks in the glass and the cracks could open up further, resulting in concentrated crack growth. Consequently, a plastic hinge occurred in the SG beams, which caused the beams to open up in two parts, see Fig. 11(a). Subsequently, the SG ruptured due to decreased flexibility of the SG at -20 °C. Due to the high bond strength of the SG at -20 °C though, as has been observed in the pull-out tests, the reinforcement remained largely attached to the glass, which enabled the beams to generate a highly plastic post-breakage response by yielding of reinforcement. However, the post-breakage strength of the SG beams remained limited to the maximum moment capacity of the plastic hinge.

Also at 60 °C the post-breakage performance of the beams decreased compared to 23 °C. Due to reduced bond strength of the SG at 60 °C, as has been observed in the pull-out tests, more excessive bond failure and consequent debonding of reinforcement occurred at the post-breakage stage. This local bond failure and consequent debonding of reinforcement caused, similar to the SG beams at -20 °C, the cracks to open up further, resulting in

concentrated crack growth. Due to this concentrated crack growth, multiple plastic hinges occurred in the beams causing the beams to open up in three parts, see Fig. 11(c). Despite progressive bond failure, the reinforcement remained largely attached to the glass, which enabled the beams to generate highly plastic post-breakage response by yielding of reinforcement. Similar to the beams tested at -20 °C, the maximum post-breakage strength of the beams at 60 °C remained limited to the maximum moment capacity of the plastic hinges.

6. Conclusions

From the pull-out tests conducted at -20 , 23 and 60 °C it is concluded that the metal-to-glass bond strength of the SG interlayer is highly temperature dependent. At high temperature levels its bond strength dramatically drops, due to reduced polymer stiffness, whereas at lower temperature levels its bond strength increases as a result of increased polymer stiffness.

Although this temperature dependency also had an effect on the structural response of the beam specimens tested at -20 , 23 and 60 °C, this effect was less dramatic as one could expect from the results of the pull-out specimens. Even at high temperature, at which the bond strength is drastically reduced, the SG interlayer could still effectively activate the metal reinforcement. Apparently the reduction in bond strength was compensated for by the relatively large bond length between glass and reinforcement within the beam specimens.

Regardless of temperature level, all beam specimens showed high-level plastic response at the post-breakage stage. It is therefore concluded that, for the beam geometry tested in the research, temperature levels within the range of -20 to 60 °C do not endanger the post-breakage and safety performance of SG-laminated reinforced glass beams. Furthermore, it is concluded that laminating a metal reinforcement to an annealed float glass beam is a feasible and very promising concept, which generates a high level of redundancy. Future research will therefore further investigate the possibilities of the SG interlayer as an intermediary between glass and various reinforcement materials. In addition to current research on the effect of different temperature levels, the effect of thermal cycling on the bond strength of the SG and the structural performance of the beam laminates will be investigated.

Acknowledgements

The authors want to gratefully acknowledge the material support of glass supplier 'Van Noordenne Groep' and interlayer producer 'DuPont' for this research. Also the support of laminating company 'Groep Leroi-Lerobel' is acknowledged. Part of this work was supported by the Fund for Scientific Research-Flanders (FWO-Vlaanderen. grant no. G.0184.07N).

References

- [1] Belis J, Depauw J, Callewaert D, Delincé D, Van Impe R. Failure mechanisms and residual capacity of annealed glass/SGP laminated beams at room temperature. *Eng Fail Anal* 2009;16:1866–75.
- [2] Delincé D, Callewaert D, Vanlaere W, Belis J. Plastic deformation of polymer interlayers during post-breakage behavior of laminated glass – partim 2: Experimental validation. *Internat J Modern Phys B* 2008;22:5447–52.
- [3] Bos FP. Safety concepts in structural glass engineering – Towards an integrated approach. Dissertation. Delft: TU Delft, 2009.
- [4] Feirabend S. In: Bos, Louter, Veer, editors. *Challenging glass*. Amsterdam: IOS Press; 2008. p. 469–78.
- [5] Belis J, Callewaert D, Delincé D, Van Impe R. Experimental failure investigation of a hybrid glass/steel beam. *Eng Fail Anal* 2009;19:1163–73.
- [6] Louter PC. Adhesively bonded reinforced glass beams. *Heron* 2007;52:31–58.
- [7] Veer FA, Rijgersberg H, Ruytenbeek D, Louter PC, Zuidema J. Conference proceedings. Tampere: Glass processing days, glaston. Finland (Oy): 2003. p. 307–10.
- [8] Bos FP. Conference proceedings. Tampere: Glass performance days, glaston Finland (Oy): 2009. p. 306–9.
- [9] Louter PC, Bos FP, Veer FA. Conference proceedings. Munich: International symposium on the application of architectural glass; 2008.
- [10] Belis J, De Visscher K, Callewaert D, Van Imper R. Conference proceedings. Tampere: Glass performance days, glaston Finland (Oy): 2009. p. 191–3.
- [11] O'Callaghan J. In: Bos, Louter, Veer, editors. *Challenging glass*. Amsterdam: IOS Press; 2008. p. 29–38.
- [12] Louter PC, Bos FP, Callewaert D, Veer FA. Conference proceedings. Tampere: Glass performance days, glaston Finland (Oy): 2009. p. 334–9.
- [13] Louter PC. Glass performance days – Conference proceedings. Tampere: glass performance days, glaston Finland (Oy): 2009. p. 139–43.
- [14] NEN-EN 572-1, Glas voor gebouwen – Basisproducten van natronkalkglas – Deel 1: Definities en algemene fysische en mechanische eigenschappen, Delft, The Netherlands, 2004.
- [15] Euro Inox, Technical table stainless steel type 304L, 2010.
- [16] Stelzer I, Bennison SJ. Conference proceedings. Munich: International symposium on the application of architectural glass. 2008.
- [17] DuPont. DuPont SentryGlas®Plus security interlayer. Technical documentation H-75287-1. s.a.
- [18] Kreher K, Natterer Jul, Natterer Joh. Timber-glass-composite girders for a hotel in Switzerland. *Struct Eng Internat* 2004;2:149–51.
- [19] Haldimann M. Fracture strength of structural glass elements – Analytical and numerical modeling, testing and design. Thèse no 3671, Lausanne: EPFL; 2006.
- [20] Bucak O, Meissner M. Trag- und Resttragfähigkeitsuntersuchungen an Verbundglas mit den Zwischenlage SentryGlas Plus – Abschlussbericht. München: AIF – Fachhochschule München; 2005.